JOURNAL OF COMPUTATIONAL PHYSICS 68, 485–500 (1987)

Unstable Fronts in a Porous Medium

J. D. SHERWOOD[1]

Etudes et Fabrication Dowell Schlumberger,
B.P. 90, 42003 St.-Etienne Cedex 1, France

Received November 1, 1985; revised March 14, 1986

A stochastic numerical scheme is used to follow the motion of a fluid interface through a porous medium. Fluid velocities are computed by Darcy's law, but the interface is advanced at a single point chosen with probability proportional to the pressure gradient. Although the expected result of each time step is proportional to that predicted by a continuum calculation, the discreteness of the scheme excites the (physical) instability which occurs when the fluid initially saturating the porous medium is displaced by a fluid of lower viscosity. The example of a five-spot oil reservoir is studied; predicted sweep efficiencies are slightly higher than experimental results, but the form of the fingering is in good qualitative agreement with experiments, even at high viscosity ratios. Grid orientation effects are low, and the effect of grid size can be reduced if care is taken to preserve trapped islands of fluid.

1. INTRODUCTION

The interface between two fluids flowing in a porous medium is unstable [1] when the more viscous fluid initially occupying the pore space is displaced by a fluid of lower viscosity. Numerical studies of the motion of such an interface must not only faithfully follow the development of the instabilities, but must also control the degree to which the instability is excited by the numerical scheme itself. In two dimensions, the equations governing Darcy flow in a porous medium are the same as those governing flow between two closely spaced parallel plates, the "Hele–Shaw cell," which has been the subject of many numerical studies [2, 3]. In particular, the development of the Saffman–Taylor instability [1] has been investigated by Tryggvasson and Aref [4], using vortex methods. The resulting fingers are indeed similar to those observed in a Hele–Shaw cell.

However, our interest here lies in flow through porous media. The fingers observed in packed bead beds [5, 6] do not resemble those in Hele–Shaw cells, even though the governing macroscopic equations are the same. Flow in the bead bed occurs through a series of discrete pores which are not present in the Hele–Shaw cell. A discrete scheme, based on diffusion limited aggregation [7], has been introduced by Paterson [8] for the case when one of the fluids is inviscid. Here we examine the extensions to finite viscosity ratios discussed in [9–12]. Finite differen-

[1] Present address: Schlumberger Cambridge Research, P.O. Box 153, Cambridge CB2 OHG, UK.

0021-9991/87 $3.00

ces are used with no attempt made to hide the discreteness of the scheme. The pressure field is calculated on the basis of Darcy's law, but the interface is advanced by discrete steps, thereby exciting the instability of the front.

In Section 2 we present the scheme and discuss its relation to the random choice method [13] for hyperbolic equations. Solutions for linear flow are briefly presented in Section 3, and in Section 4 we consider the classic numerical problem of the five-spot oil reservoir.

2. The Numerical Scheme

We assume that the rock is saturated either with the fluid initially present, (fluid 1, with viscosity μ_1), or with the injected fluid (fluid 2). The fluid velocity $\mathbf{u}$ is given by Darcy's law

$$\mathbf{u} = -\frac{k}{\mu}\nabla p,$$

where p is the pressure and k is the permeability of the rock. We consider miscible displacement in which interfacial tension between the fluids is ignored, and in which k is identical for the two fluids; henceforth k is assumed uniform and set equal to 1. The fluids are assumed incompressible. Hence

$$\nabla \cdot \mathbf{u} = 0 \qquad \text{and} \qquad \nabla^2 p = 0,$$

except at injection points. The front between the two fluids is convected with the fluid, and is thus determined by an advection equation

$$\frac{\partial c}{\partial t} + \nabla \cdot (\mathbf{u}c) = 0,$$

where c takes the values 1 or 0 in the injected fluid and in the original fluid, respectively. Note that we ignore dispersion. This would lead to mixing of the fluids, to intermediate values of c and to intermediate values of the viscosity, which would become a function of c.

When the injected fluid is less viscous than the fluid it displaces ($\mu_2 < \mu_1$), the front between the fluids is unstable and fingers of injected fluid will invade the rock. The fingering will occur on all length scales, though the smallest fingers will be destroyed by the effects of dispersion and molecular diffusion. In the simulations presented here, the cut-off at small length scales is at the size of the finite difference grid.

With incompressible fluids, the pressure satisfies the Laplace equation and the front advances with the fluid velocity $\propto \nabla p$. These same equations govern the flux of Brownian particles following a random walk [14], and Paterson [8] has made use of this analogy to model flow in porous media. If the particles encounter a growing

aggregate, they stick to it: the aggregate represents the body of injected fluid advancing into the rock. However, the aggregate corresponds to an iso-potential. This analogy with Diffusion Limited Aggregation [7] therefore only holds when one of the fluids is inviscid. It is this restriction which we have sought to remove.

We study two dimensional (x, y) flow, using a square grid for the finite difference scheme. Within each of the zones occupied by a single fluid, the fluid velocity (u, v) between blocks (i, j), $(i+1, j)$ is

$$u_{i+1/2} = \frac{p_i - p_{i+1}}{\mu}.$$

We consider the entire rectangle $(i-\frac{1}{2}, i+\frac{1}{2}) \times (j-\frac{1}{2}, j+\frac{1}{2})$ to be occupied by fluid 1 if the point (i, j) is so occupied. The interface between the fluids therefore lies midway between gridpoints, and is parallel to either the x or y axis. Continuity of velocity normal to the interface implies

$$u_{i+1/2} = \frac{2(p_i - p_{i+1})}{\mu_1 + \mu_2}$$

if the two gridblocks contain different fluids. Incompressibility then leads to the standard five point Laplacian operator within each fluid, with a modified form at the interface; the pressure field is determined by Gauss–Seidel iteration.

Once the fluid velocity is known, we can then solve the advection equation for the position of the interface between the two fluids. A classical numerical scheme would advance the entire interface by a distance proportional to the fluid velocity (and hence to the pressure gradient). Rather then adopt this continuum approach, we continue with a discrete scheme in which the injected fluid 2 advances into, and fills, a single elementary rectangle of the finite difference grid at each time step. One segment of the interface is chosen with probability proportional to the modulus of the local normal pressure gradient $|\mathbf{n} \cdot \nabla p|$, and is advanced in the direction of $\mathbf{n}(\mathbf{u} \cdot \mathbf{n})$. The expected advance is therefore proportional to that predicted by a classical scheme. However, a classical scheme would also allow arbitrary orientation of the interface, and hence an arbitrary direction of motion. Finally, we note that in the implementation considered here, fluid 2 always replaces fluid 1, and those portions of the interface which might move in the opposite direction are frozen (before the pressure gradients and corresponding probabilities are computed). This restriction has been relaxed in a somewhat similar scheme by DeGregoria [10], while King and Scher [9] have shown how intermediate saturations and relative permeabilities may be introduced.

An alternative approach would be to solve the hyperbolic equations for the advancing interface by means of the random choice method [13, 15–21]. In this method the expected advance is also proportional to that predicted by a classical scheme, and the step interface between the fluids is preserved by sampling the exact solution of a one-dimensional Riemann problem. An important difference is that in

a
INJECTED VISCOSITY=1.000
INITIAL VISCOSITY=10000.001
INITIAL SEED=4039
NUMBER OF STEPS=3000
NI=160
NJ=160
DENSITY
1.0
0.0
0 10 20 30 40 50 60 70 80 90 100 110 120 130 140 150 160
b
INJECTED VISCOSITY=1.000
INITIAL VISCOSITY=10.000
INITIAL SEED=4039
NUMBER OF STEPS=3000
NI=160
NJ=160
DENSITY
1.0
0.0
0 10 20 30 40 50 60 70 80 90 100 110 120 130 140 150 160

581/68/2-16

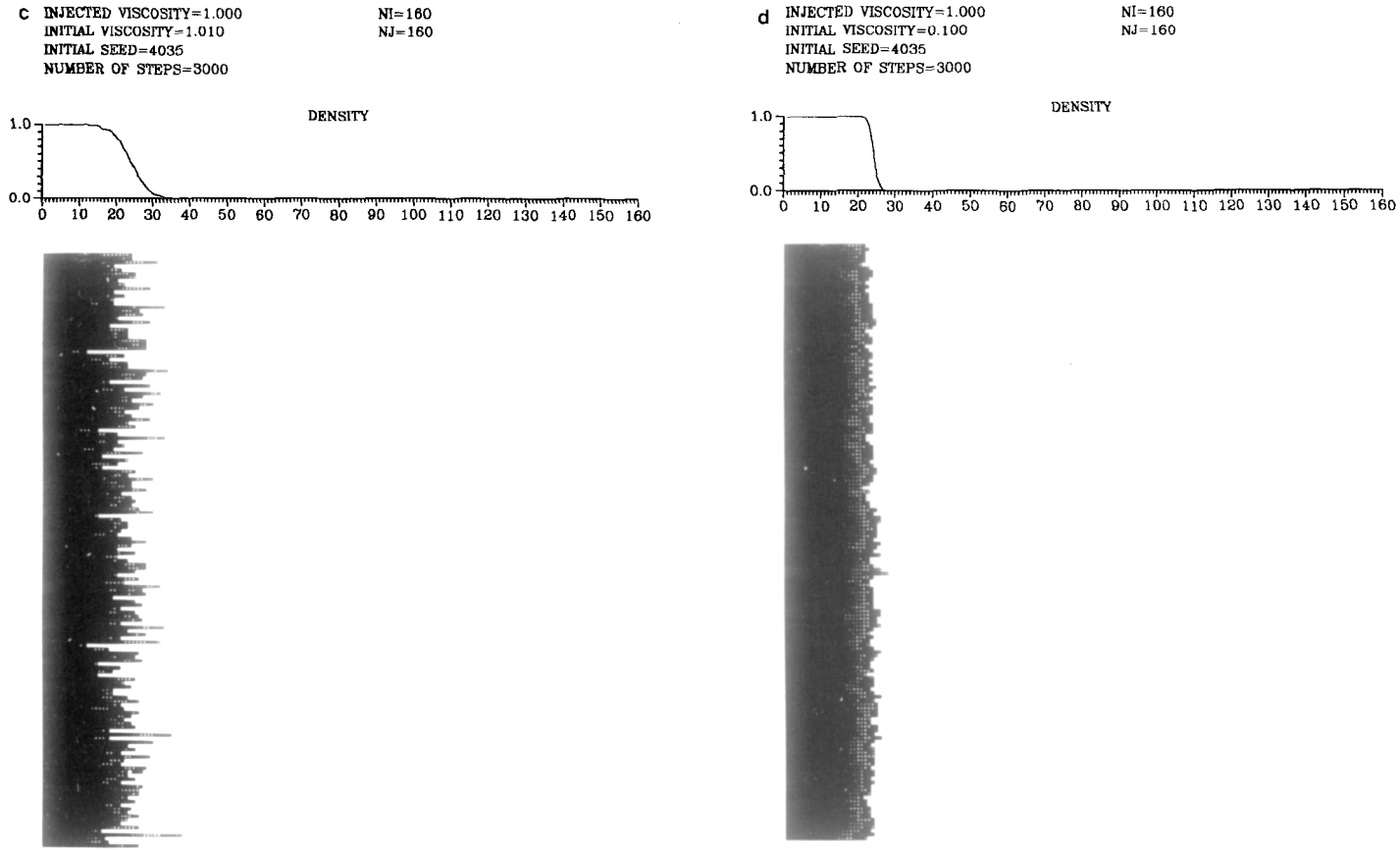

FIG. 1. Linear flooding after injection of 3000 grid blocks. Viscosity ratio $\mu_1/\mu_2 =$ (a) 10^4; (b) 10; (c) 1.01; (d) 0.1.

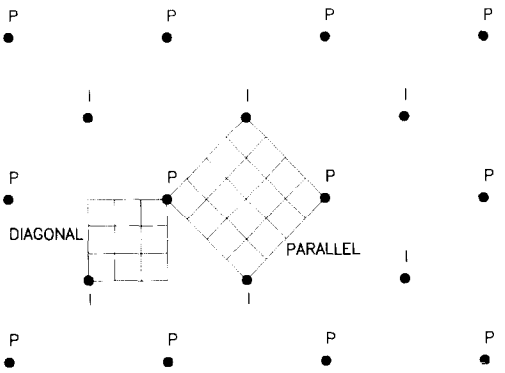

FIG. 2. The five-spot well pattern.

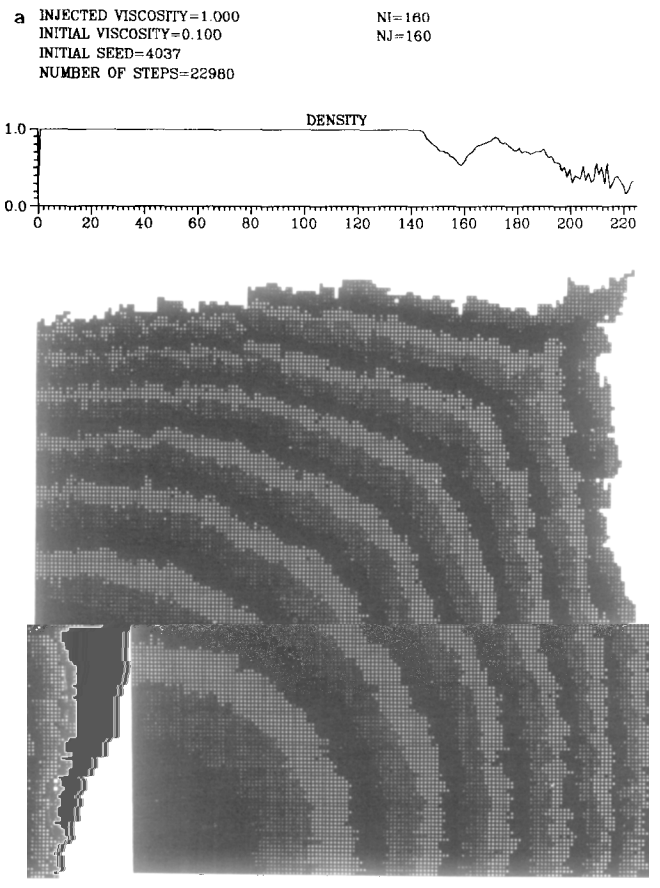

FIG. 3. Simulations of the displacement fronts at breakthrough, using a diagonal grid. Viscosity ratio $\mu_1/\mu_2 =$ (a) 0.1; (b) 1.01; (c) 100.

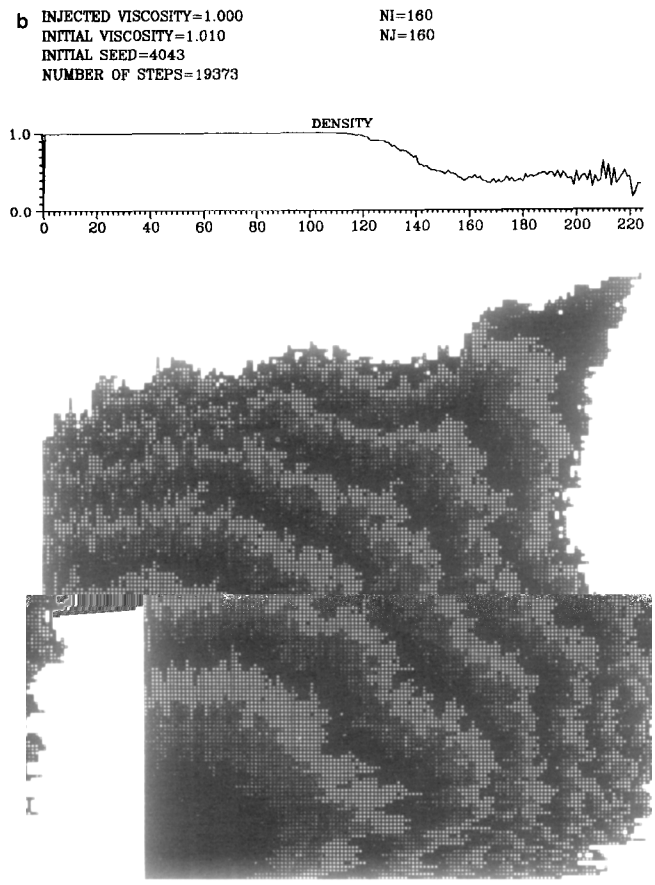

FIG. 3—*Continued.*

In the results presented here the advance always occurs at one and only one point. In the random choice method the number of points of advance at each time step will be small when the time step is short. However, this is precisely the condition which maximises the standard deviation of the results obtained [13]. The results of Sections 3 and 4 can is this sense be regarded as an extreme case of the random choice method.

The random numbers used here also serve to excite the instability, and are sampled throughout the course of the simulation. The randomness of flow in real porous media has been studied both on the macroscopic scale [22, 23] and on the scale of pores and capillaries [24–26]. However, such calculations are completely deterministic once the properties of the media have been assigned.

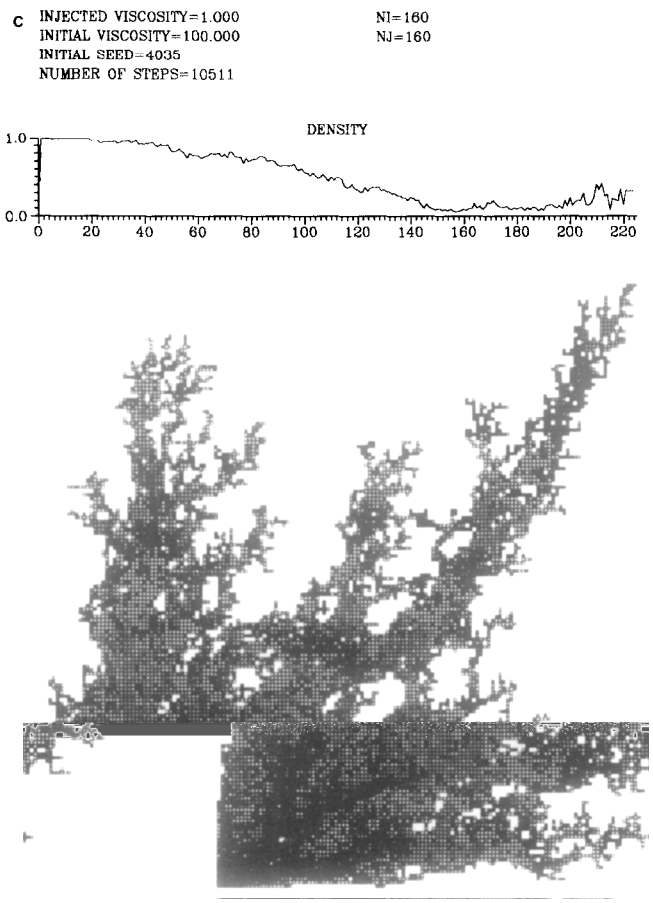

FIG. 3—*Continued.*

Although the results can appear very similar to those presented here, the links (if any) between the simulations are as yet unclear.

3. LINEAR FLOODING

Figure 1 shows the results of calculations for linear flooding. Flow is from left to right, and black regions represent injected fluid. The left- and right-hand boundaries are held at constant pressure; Neumann boundary conditions are applied on the remaining two sides. The interface between the two fluids is initially five blocks in from the injection edge in order to reduce edge effects. Gauss–Seidel iteration is used to solve for the pressure. Up to six iterations are performed on the 9×9 blocks

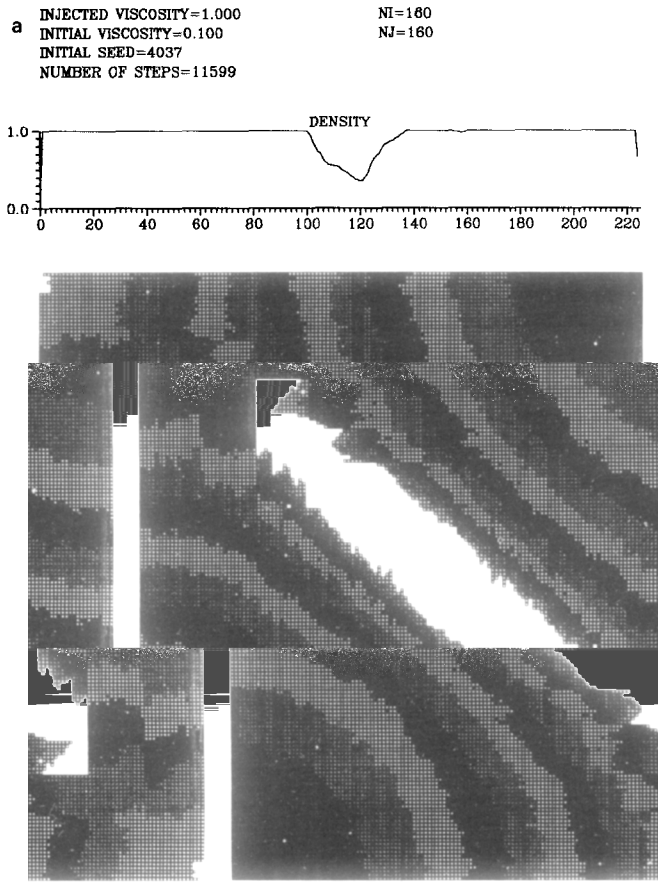

FIG. 4. Simulations of the displacement fronts at breakthrough, using a parallel grid. Viscosity ratio $\mu_1/\mu_2 =$ (a) 0.1; (b) 1.01; (c) 100.

surrounding the point at which the interface has advanced, followed by sweeps over the entire array until the sum of the squares of residuals is sufficiently small (usually $10^{-8} \times$ number of gridpoints). The number of iterations is typically between 1 and 15. A single iteration suffices if the interface has advanced in a region with low pressure gradients, or if the viscosity ratio is close to unity. When the grid is of size 160×160, 2000 time steps take approximately one hour on a VAX 785. Other studies of linear flooding, using the random choice method (but with intermediate saturations and relative permeabilities) are reported in [15–17].

In figure 1a the viscosity ratio $\mu_1/\mu_2 = 10^4$. The interface is unstable. The growing fingers exhibit the sideways branching observed, on the microscopic scale, in etched glass networks of pores and capillaries [24]. In Fig. 1b–d the viscosity ratio is reduced to 10, 1.01, and 0.1. The same volume of fluid, 3000 grid blocks, has been

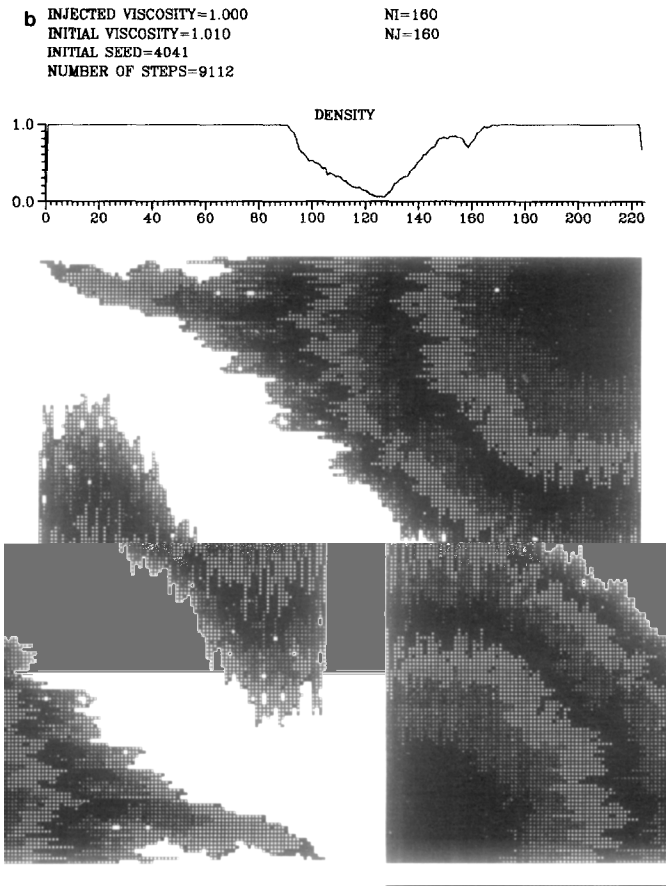

FIG. 4—*Continued.*

injected in each case. In Fig. 1d the front is stable, with random fluctuations which do not grow. When the viscosity ratio is unity (Fig. 1c) the pressure gradient is constant throughout the simulation. Each point of the interface has an equal probability β of motion. If we relax our restriction of a single point of advance, we have a series of independent Bernouilli trials. For each value of y, the x co-ordinate of the front has a binomial distribution, with mean $\bar{x} = \beta t$, variance $\overline{(x - \bar{x})^2} = \beta t(1 - \beta)$. We have introduced a degree of numerical dispersion, and lateral diffusion would also be present if the flow was not aligned with the coordinate axes. Simulations of radial flow [12] show similar grid orientation effects when the two viscosities are equal. However, these effects disappear at other viscosity ratios.

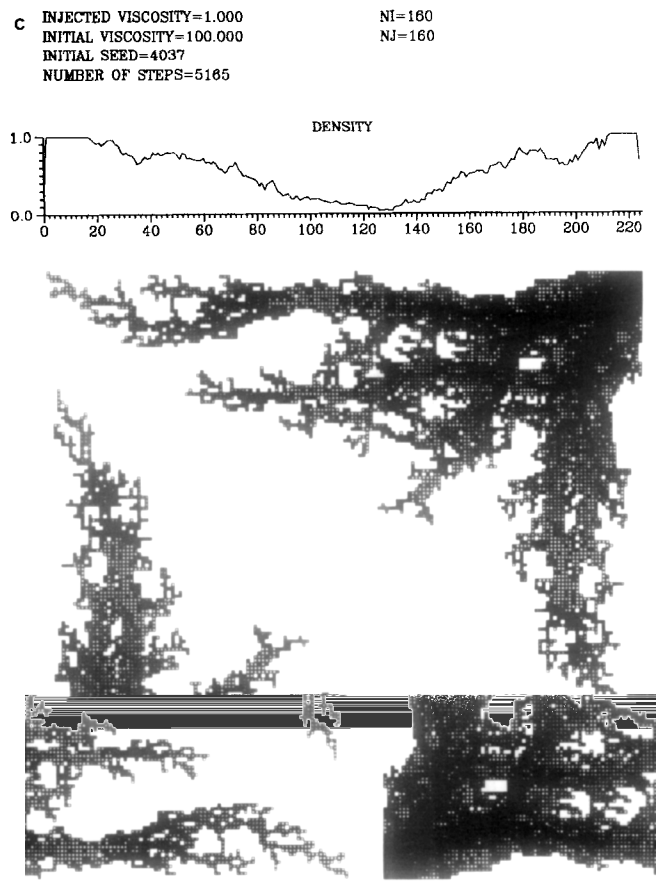

FIG. 4—*Continued.*

fusion Limited Aggregation that grid effects are still present even when $\mu_2 = 0$ [27], though the effect is so small that it can only be observed after many ($\sim 3 \times 10^4$) time steps.

These results for linear flow have proved difficult to quantify [11]. We therefore turn to the five-spot oil reservoir, which can be characterized by a single figure, the sweep efficiency S at the moment of breakthrough.

4. THE FIVE-SPOT OIL RESERVOIR

The "five-spot" well pattern is shown in Fig. 2. Water (or some other fluid) is injected at the wells marked *I*, and oil (we hope) is recovered at the production

wells P. By symmetry we need only consider one repeating unit of the well pattern. However, as is shown in Fig. 2, there are two natural alignments for a rectangular computational grid. (In addition, a conformal transformation is frequently employed to obtain an "elliptic" grid [20, 28, 29], which we shall not consider here.) The results in Fig. 3 are computed on a diagonal grid. Thus the bottom left-hand corner of each plot corresponds to an injection well, the top right-hand corner to a production well. These points are held at constant pressure $p = 1$, 0, respectively; elsewhere the pressure gradient normal to the boundary is zero. Figure 3 shows the zones saturated by the injected fluid at the moment of breakthrough, when fluid 2 reaches the production well. Miscible five-spot flooding experiments have been performed on a laboratory scale in sand beds [30] and in packed beds of glass beads [31]. There is a marked qualitative agreement between the experimentally observed fingering and that predicted by simulations, over the whole range of stable and unstable viscosity ratios.

The five-spot problem is a classical test for reservoir simulations [18–21, 28, 29, 32–39]. Saturations of the initial and injected fluid are usually allowed to vary continuously between 0 and 1, for both miscible and immiscible fluids. However, Glimm et al. [29] have studied miscible fluids with zero diffusion, using front tracking. To reproduce the fingering which is observed experimentally [30, 31], they start with a perturbed interface between the fluids. The fingering in Fig. 3 is excited by the numerical method itself. Note that in Fig. 3a, a numerical instability occurs when the front approaches the no-flux boundary. Although the initial fluid

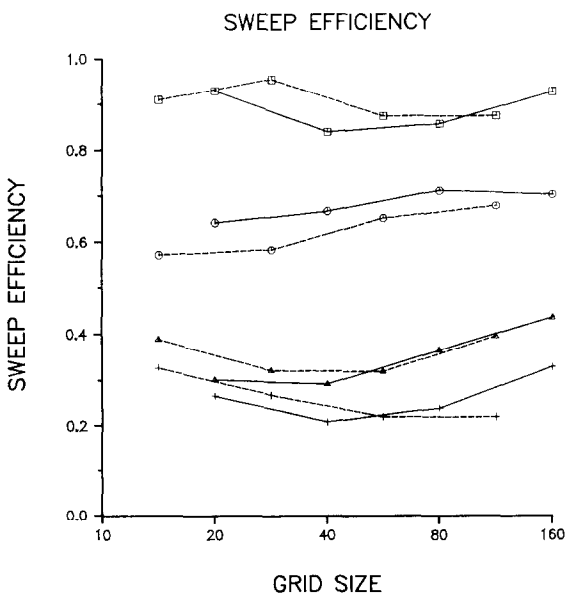

FIG. 5. The sweep efficiency S, as a function of the grid size, at viscosity ratios $\mu_1/\mu_2 = \square$, 0.1; ○, 2.0; △, 10^2; +, 10^4. Solid lines are results on diagonal grids, broken lines on parallel grids.

can be displaced by the injected fluid, the reverse is not permitted by the scheme at present. A perturbation of the interface cannot therefore be swept along the interface towards the production well.

Numerical studies of the five-spot problem can be affected by grid orientation (see [39] for a review). Figures 4a–c are computed on a parallel grid, with injection at the bottom left- and top right-hand corners. A convenient method of quantifying the results is to compute the sweep efficiency S, the fraction of fluid 1 produced up to the moment of breakthrough. S is shown in Fig. 5 as a function of grid size, for four different viscosity ratios. The solid lines correspond to diagonal grids of size 20×20, 40×40, 80×80 and 160×160. The broken lines correspond to parallel grids, with the same sizes, though the results are displaced since, as can be seen in Fig. 2, a diagonal grid requires only half as many blocks to achieve the same resolution. There is no significant difference between the results.

Note that different series of random numbers produce different results for S. Each point in Figs. 5–7 is therefore an average over five runs. The standard deviations are usually of the order of ± 0.03, but are up to ± 0.08 on the smaller grids and parallel grids.

In Fig. 6 we show results, on a diagonal grid, as a function of viscosity ratio. The four curves correspond to the four grid sizes. Although the sweep efficiency is generally higher on the larger grids, the curves cross and the trend is not consistent. Also shown are the experimental results of Habermann [30] for the volumetric sweep efficiencies. These are in general lower than the computed results. An anaytic

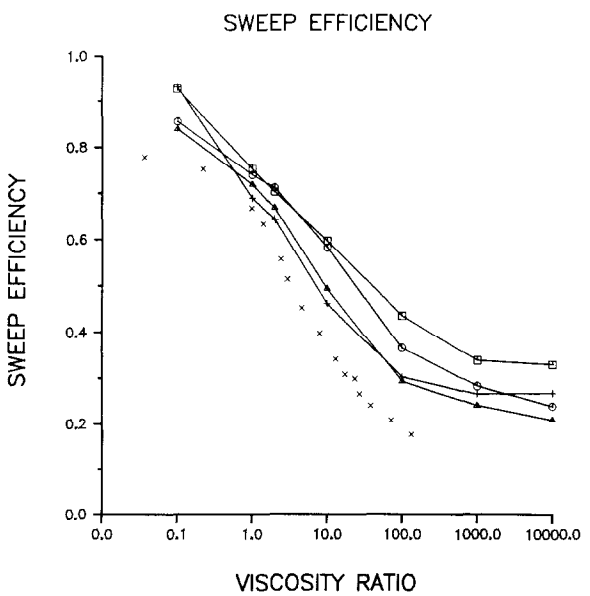

FIG. 6. The sweep efficiency S, as a function of the viscosity ratio μ_1/μ_2. Diagonal grid, size: □, 160×160; ○, 80×80; △, 40×40; +, 20×20. ×, Habermann's [30] experimental values.

result, $S = 0.72$ is available [28] when the viscosity ratio is unity, while Paterson [8] obtained, *via* simulations of diffusion limited aggregation, a sweep efficiency 0.11 at an infinite viscosity ratio.

ded by fluid 2, are not preserved. In two dimensions fluid 1 should not be able to escape: nevertheless the scheme allows fluid 2 to slowly fill up the island. This can be corrected by extra care, and Fig. 7 shows results for S when islands are preserved, but not allowed to move with the surrounding fluid. The effect of grid size is markedly reduced from that in Fig. 6. Conservation of volume is more correctly respected, and the scheme is therefore more consistent. However, the curves still cross each other, and cannot be used to obtain the scaling with grid size observed in [9, 10].

Even when volume is correctly conserved, there is still a difference between predicted and experimental sweep efficiencies. Moreover, the form of the viscous fingers at breakthrough (Fig. 8, at a viscosity ratio 100) now bears *less* resemblance to the experimentally observed fingers [30, 31]. The experimental points on Figs. 6 and 7 are volumetric sweep efficiencies. If S is measured on the basis of the area swept at breakthrough, the values obtained are higher. The bead bed used by Leftwich [31] had dimensions $210 \times 210 \times 5$ mm, and was only five layers of beads thick. Even so fingering occurred within the depth of the bed, the full thickness of which was not swept. At viscosity ratios $\mu_1/\mu_2 = 1.0$, 2.0, 10 and 100 Leftwich

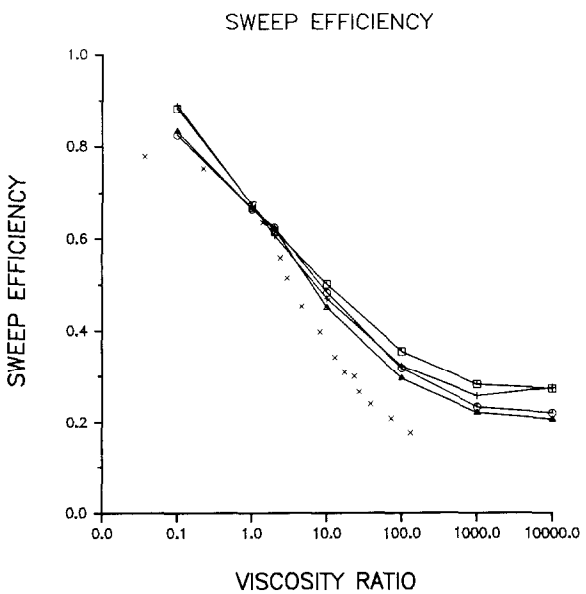

FIG. 7. The sweep efficiency S, as a function of the viscosity ratio μ_1/μ_2, when islands are preserved. Diagonal grid, size: □, 160×160; ○, 80×80; △, 40×40; +, 20×20. ×, Habermann's [30] experimental values.

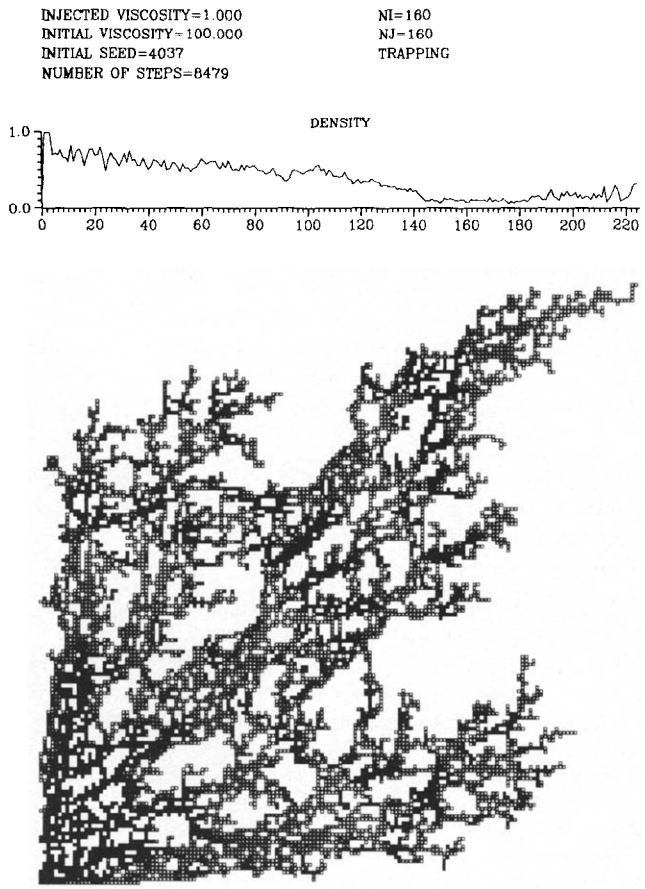

FIG. 8. The displacement front at breakthrough, using a diagonal grid, with trapped islands of the original fluid preserved. Viscosity ratio $\mu_1/\mu_2 = 10^2$.

obtained volumetric sweep efficiencies 0.6, 0.58, 0.35 and 0.2, while the areal sweep efficiencies were 0.77, 0.73, 0.55 and 0.65. A purely two-dimensional solution neglects variations across the depth of the bed, and must be regarded with caution when the interface is unstable. Despite these problems, the form of the fingering produced by the simulations is sufficiently similar to the experimentally observed fingers even at high viscosity ratios of order 100, to make the scheme of interest.

REFERENCES

1. P. G. SAFFMAN AND G. I. TAYLOR, *Proc. R. Soc. London Ser. A* **245**, 312 (1958).
2. J. W. MCLEAN AND P. G. SAFFMAN, *J. Fluid Mech.* **139**, 455 (1981).
3. G. H. MEYER, *J. Comput. Phys.* **44**, 262 (1981).

4. G. TRYGGVASON AND H. AREF, *J. Fluid Mech.* **136**, 1 (1983).
5. L. PATERSON, *Powder Tech.* **36**, 513 (1983).
6. L. PATERSON, *Phys. Fluids* **28**, 26 (1985).
7. T. A. WITTEN AND L. M. SANDER, *Phys. Rev. Lett.* **47**, 1400 (1981).
8. L. PATERSON, *Phys. Rev. Lett.* **52**, 1621 (1984).
9. M. J. KING AND H. SCHER, *Probabilistic Stability Analysis of Multiphase Flow in Porous Media*, paper SPE 14366, presented at the 60th Annual Technical Conference of SPE, Las Vegas, 1985.
10. A. J. DEGREGORIA, *Phys. Fluids* **28**, 2933 (1985).
11. J. D. SHERWOOD AND J. NITTMANN, *J. Phys. (Paris)* **47**, 15 (1986).
12. J. D. SHERWOOD, *J. Phys. A: Math. Gen.* **19**, L195 (1986).
13. A. J. CHORIN, *J. Comput. Phys.* **22**, 517 (1976).
14. L. KADANOFF, *J. Statist. Phys.* **39**, 267 (1985).
15. J. GLIMM, D. MARCHESIN, AND O. MCBRYAN, *Commun. Math. Phys.* **74**, 1 (1980).
16. J. GLIMM, D. MARCHESIN, AND O. MCBRYAN, *J. Comput. Phys.* **39**, 179 (1981).
17. A. J. CHORIN, *Commun. Math. Phys.* **91**, 103 (1983).
18. N. ALBRIGHT, P. CONCUS, AND W. PROSKUROWSKI, *Numerical Solution of the Multi-dimensional Buckley–Leverett Equation by a Sampling Method*, paper SPE 7681, presented at the 5th SPE Reservoir symposium, Denver, 1979.
19. N. ALBRIGHT AND P. CONCUS, in *Fluid Mechanics in Energy Conservation*, edited by J. D. Buckmaster, (SIAM, Philadelphia, 1980), p. 172.
20. J. GLIMM, D. MARCHESIN, AND O. MCBRYAN, *Commun. Pure Appl. Math.* **34**, 53 (1981).
21. J. A. SETHIAN, A. J. CHORIN, AND P. CONCUS, *Numerical Solution of the Buckley–Leverett Equations*, paper SPE 12254, presented at the SPE Reservoir simulation symposium, San Fransisco, 1983.
22. G. DAGAN, *J. Fluid Mech.* **145**, 151 (1984).
23. L. SMITH AND F. W. SCHWARTZ, *Water Resour. Res.* **16**, 303 (1980).
24. R. LENORMAND AND C. ZARCONE, *Physico-Chemical Hydrodynamics* **6**, 497 (1985).
25. R. CHANDLER, J. KOPLIK, K. LERMAN, AND J. F. WILLEMSEN, *J. Fluid Mech.* **119**, 249 (1982).
26. J.-D. CHEN AND D. WILKINSON, *Phys. Rev. Lett.* **47**, 1892 (1985).
27. R. C. BALL AND R. M. BRADY, *J. Phys. A: Math. Gen.* **18**, L809 (1985).
28. H. J. MOREL-SEYTOUX, *Trans. A.I.M.E.* **237**, 217 (1966).
29. J. GLIMM, E. ISAACSON, D. MARCHESIN, AND O. MCBRYAN, *Adv. Appl. Math.* **2**, 91 (1981).
30. B. HABERMANN, *Trans. A.I.M.E.* **219**, 264 (1960).
31. I. LEFTWICH, M. Eng. project report, Heriot–Watt University, 1985 (unpublished).
32. M. R. TODD, P. M. O'DELL, AND G. J. HIRASAKI, *Trans. A.I.M.E.* **253**, 515 (1972).
33. K. H. COATS, W. D. GEORGE, C. CHU, AND B. E. MARCUM, *Trans. A.I.M.E.* **257**, 573 (1974).
34. J. L. YANOSIK AND T. A. MCCRACKEN, *Trans. A.I.M.E.* **267**, 253 (1979).
35. L. C. YOUNG, *Trans A.I.M.E.* **271**, 115 (1981).
36. J. GLIMM, B. LINDQUIST, O. A. MCBRYAN, B. PLOHR, AND S. YANIV, *Front Tracking for Petroleum Reservoir Simulation*, paper SPE 12238, presented at the SPE Reservoir simulation symposium, San Fransisco, 1983.
37. R. E. EWING, T. F. RUSSELL, AND M. F. WHEELER, *Simulation of Miscible Displacement Using Mixed Methods and a Modified Method of Characteristics*, paper SPE 12241, presented at the SPE Reservoir simulation symposium, San Fransisco, 1983.
38. L. C. YOUNG, *Comput. Meth. Appl. Mech. Eng.* **47**, 3 (1984).
39. G. R. SHUBIN AND J. B. BELL, *Comput. Meth. Appl. Mech. Eng.* **47**, 47 (1984).